

Supplementary Information

Persistent Drought Monitoring Using a Microfluidic-Printed Electro-Mechanical Sensor of Stomata *in planta*

Volodymyr B. Koman¹, Tedrick T. S. Lew¹, Min Hao Wong¹, Seon-Yeong Kwak¹, Juan P. Giraldo² and
Michael S. Strano^{1*}

* *Corresponding author:* strano@mit.edu

Note 1. Electrical response without pillars.

Under illumination, patterned stomata have similar opening and closing dynamics as compared to non-patterned ones, suggesting that the ink has no effect on them (Fig. S12, bottom). Simultaneous electrical measurements across the patterned stoma demonstrated a sudden jump in the electrical resistance during stoma opening, which we attribute to the loss of contact of the printed stripe (Fig. S12, top). Contrary to expectation, when the stoma closes the electrical contact is not resumed. This is probably because the stoma does not close in exactly the same manner, making it difficult for the thin printed layer to recover its initial contact. Out of 69 wired stomata, only 10 demonstrated conductive patterns as in Fig. S12, while others did not show any resistance modulation (Fig. S13). Such unreliability motivated us to add conductive micropillars to improve electrical contact.

Note 2. Impedance spectroscopy.

Electrical measurements performed on leaf surface contain significant noise. In an effort to minimize this noise, we performed measurements with frequency envelopes (Fig. S14). This did not bring any noticeable improvement. To further understand leaf electrical behavior, we performed impedance spectroscopy measurements using Gamry Interface 1000A: first, on a bare leaf and then on a leaf coated with ink (Fig. S15). The bare leaf shows resistive behavior (due to mesophyll liquids) with interlayer capacitance between mesophyll and epidermis (extracted parameters are $R \approx 4 \text{ MOhm}$, $C \approx 0.1 \text{ nF}$). A leaf coated with ink behaves as a pure resistor because of high ink conductivity. Imaginary resistance increases slightly due to the skin effect.

When a stoma opens, electrodes placed on guard cells form a capacitor. We further discuss whether it is possible to electrically measure this capacitance, giving us access to stomata size. Taking electrode cross-sections to be $5 \times 5 \text{ } \mu\text{m}^2$, we estimate a gap capacitance in between electrodes to be 20 aF for 10 nm distance (2 aF for 100 nm). Such values are, in principle, possible to measure using state-of-the-

art devices, but these devices are sensitive to perturbations and not compatible with in-field measurements. Moreover, interlayer capacitance has much larger values, making it impossible to resolve gap capacitance.

Note 3. Group stomata response.

To understand stomatal behavior under low light illumination and to explore the possibility of having multiple SAEM on the same leaf, we study whether stomata act individually or synchronously. While stomata on isolated epidermis respond independently to blue light [1], there is still much discussion about stomata behavior on a leaf [2, 3]. Although, at the first sight, guard cells should act independently, neighboring mesophyll cells can influence stomatal apertures by affecting the composition of apoplastic fluid, malate and the intracellular CO₂ concentrations [4, 5]. To test this effect, we illuminated a limited leaf area while keeping the rest of the plant in the dark (Fig. S16a). If the illumination spot covers the whole leaf (corresponds to $d = 5$ cm), stomata on this leaf open (Fig. S16b). Interestingly, stomata open even if the opposite side of the leaf is illuminated. This is because photosynthesis launches a chain reaction to generate malate, an important plant anion, which spreads across plant mesophyll and causes stomata to partially open [4]. If the illumination spot is reduced to 1.5 mm circle, stomata in this region remained closed. This is probably an effect of neighboring mesophyll cells, which remain in the dark and are, therefore, closed. If we repeat the same experiment when the plant is under ambient light, i.e. stomata are partially open, results differ (Fig. S16c). Specifically, stomata in the 1.5 mm illuminated region partially open, while smaller illumination spots still have no effect on stomata aperture. These results indicate that peace lily stomatal response depends mostly on the neighboring cells illumination and has strong collective component.

Note 4. Transferring microelectrodes onto leaf surface.

We further develop another variation of microelectrodes for stoma readout. Instead of ink-printed electrodes, we first fabricated 0.3 μm thick SU-8 electrodes using photolithography, and coat them with the conductive ink (Fig. S17). Then these electrodes are covered with PMMA layer and lifted off from a substrate, by dissolving SiO_2 in KOH for 2h (Fig. S18). Floating electrodes are picked up by a PDMS support and coated with PVA. Next, PMMA layer is dissolved by acetone. Microelectrodes, supported by the PVA layer, are transferred on a leaf surface and aligned on a stoma. Finally, the PVA layer is washed away with water, leaving electrodes on a leaf surface (Fig. S19).

To wire a stoma, electrode transfer process needs to be repeated twice (Fig. S20a, c). The operational principle of this system remains similar to the printed circuit (Fig. S20b). We further confirmed that our electrodes do not interfere with stoma by measuring stoma response to light in three consecutive light on/off cycles, and comparing it to an unpatterned stoma (Fig. S20d). Simultaneous electrical measurements demonstrate electrical jumps during stomatal openings and closures (Fig. S20e). Extracted delay times (Fig. S20f, 24 min for opening and 36 min for closing) correspond to stomatal contact loss at approximately 0.5 μm aperture opening. The latter value could be tuned by the proper electrode alignment. Also note that resistance measurements contain much less noise as compared to the carbon nanotubes ink, because of much better mechanical stability.

Supporting Figures

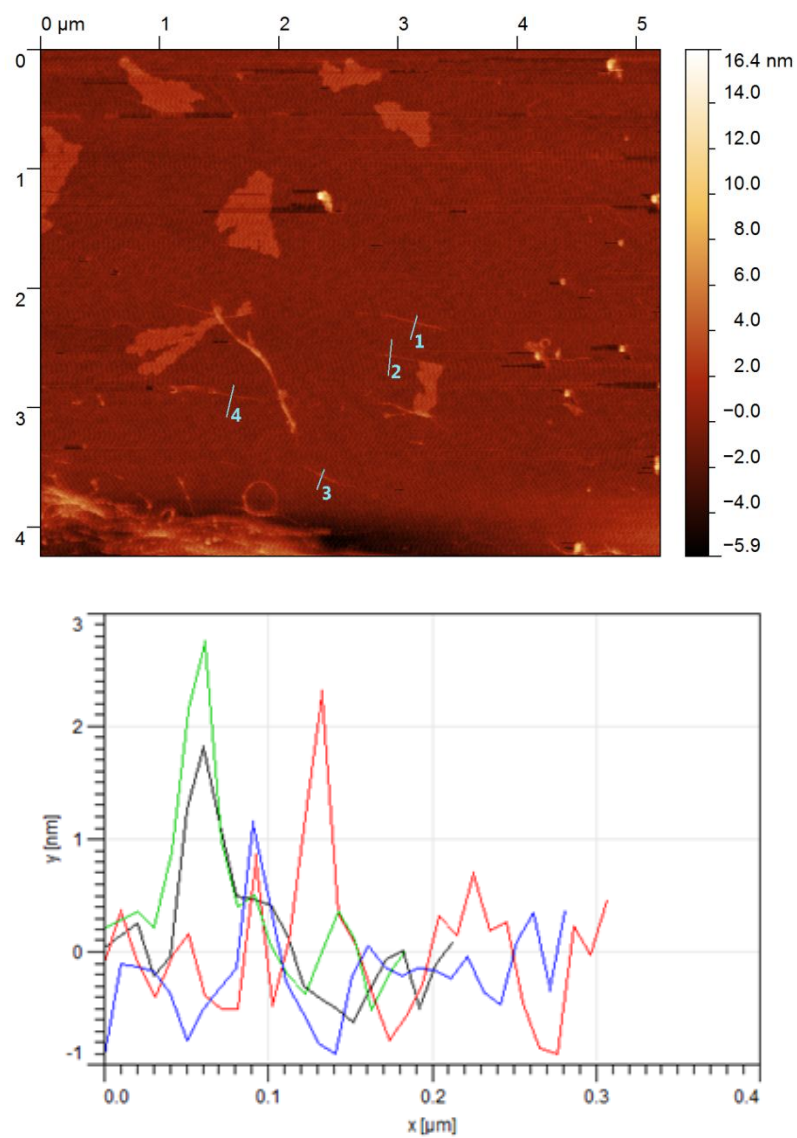


Figure S1. Atomic force microscopy (AFM) surface map demonstrating individual carbon nanotubes from AC100 ink on SiO₂ surface.

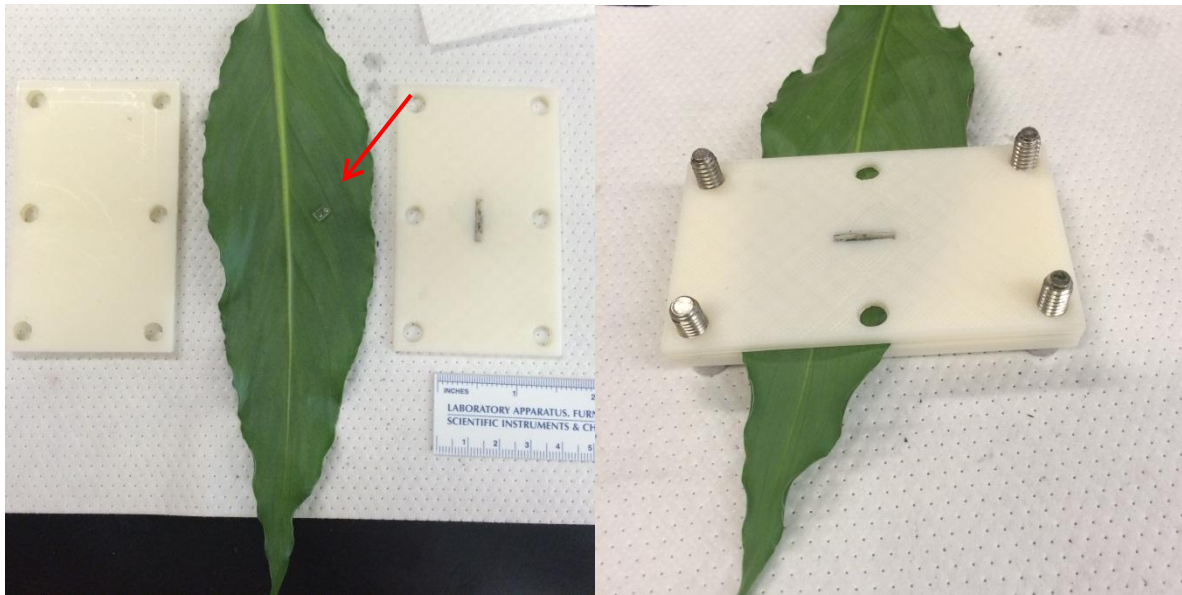


Figure S2. A set for microfluidic leaf printing (left – disassembled and right – assembled): a microfluidic chip placed between leaf veins and two plastic holders for clamping. The top holder has an opening to insert ink into the microfluidic chip after clamping. Red arrow points on microfluidic chip. (Bottom) Microfluidic chip is aligned on top leaf surface using XYZ translational stage.

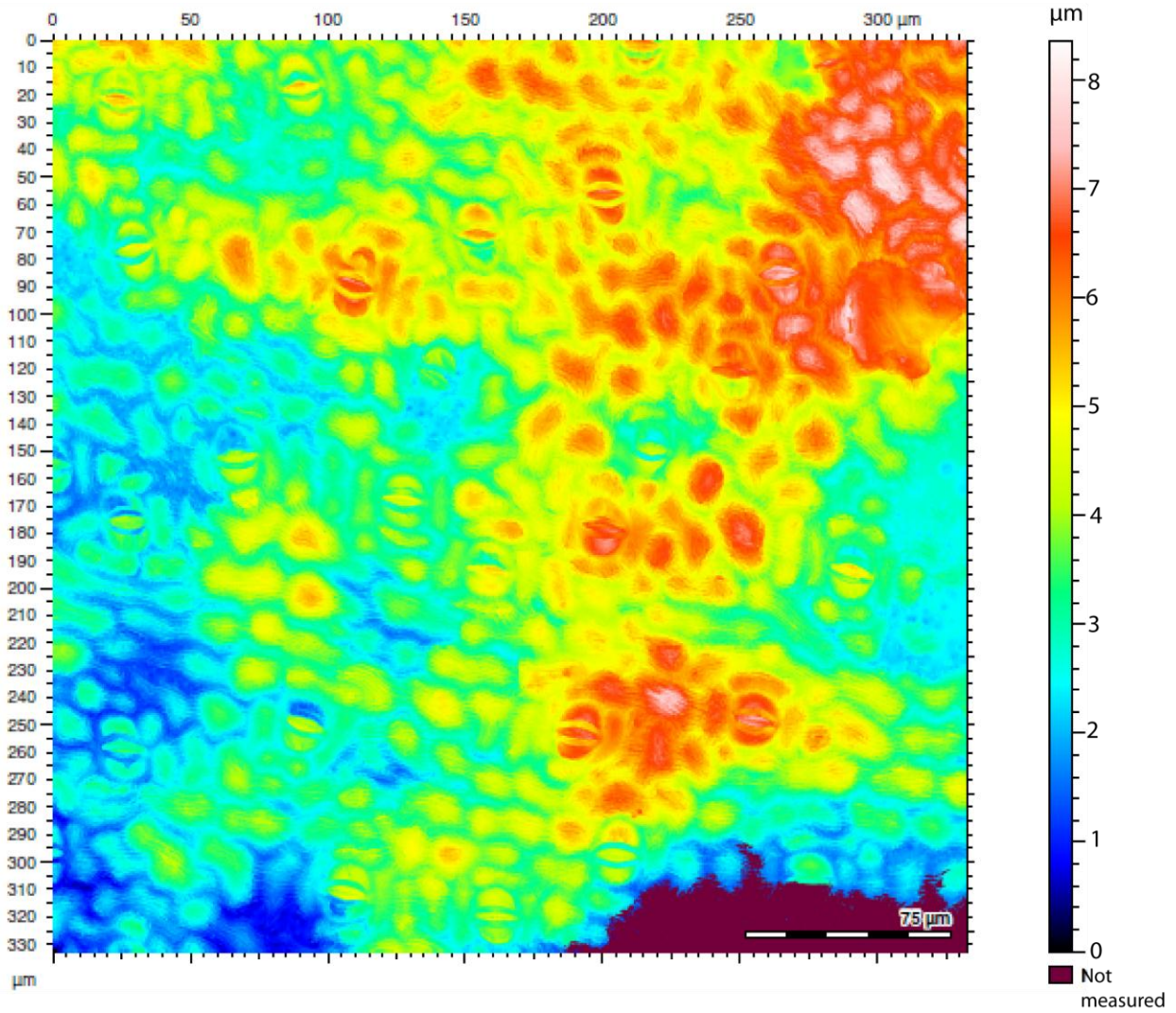


Figure S3. A typical profile height map of peace lily abaxial leaf surface.

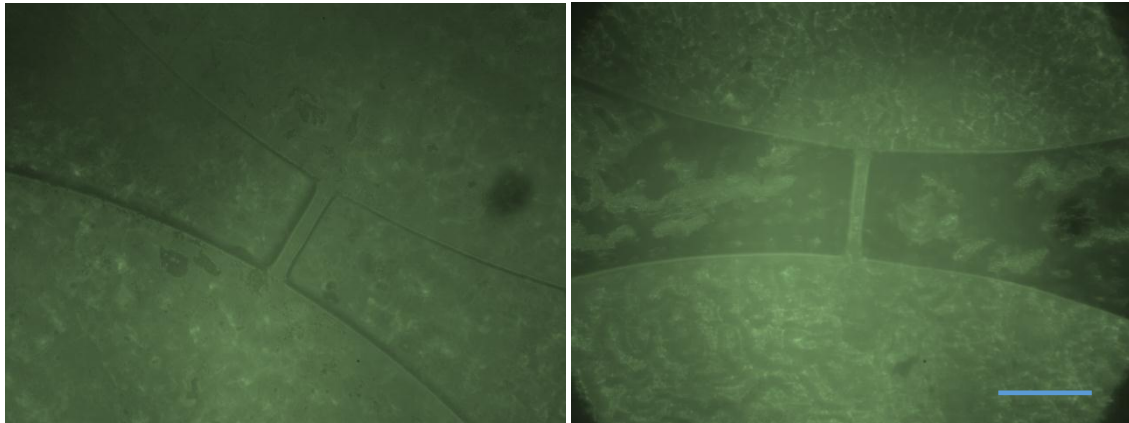


Figure S4. Comparison between bad (left, PDMS seems transparent because there is an air gap between the chip and the leaf) and good adhesion of PDMS and leaf surface. Scale bar: 100um.

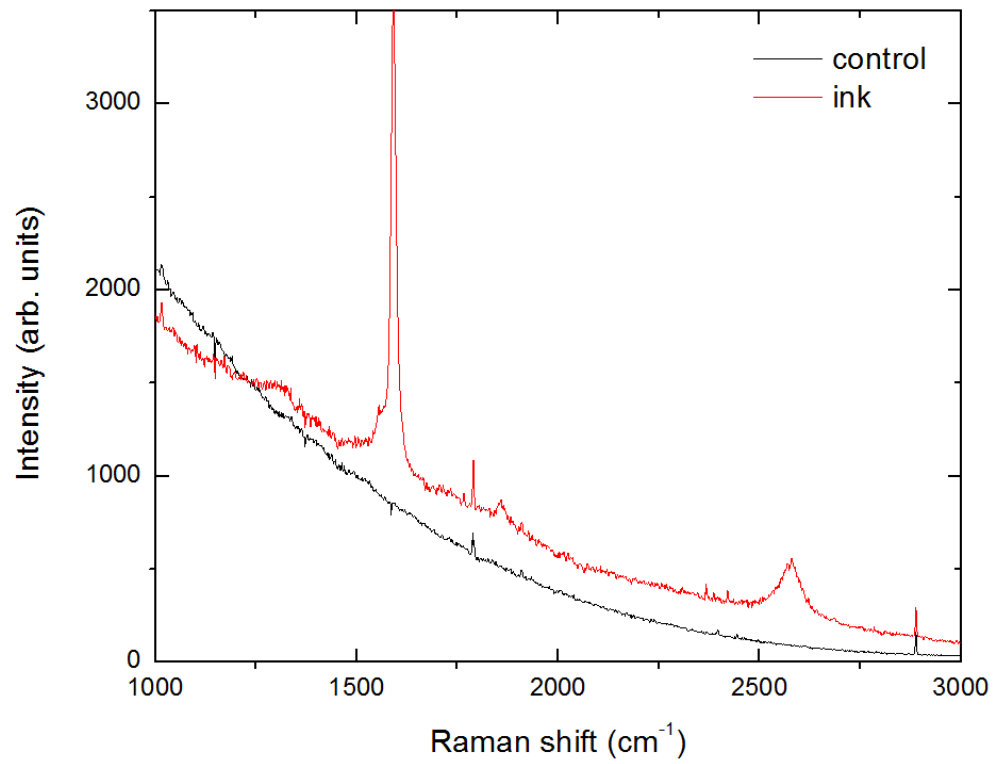


Figure S5. Typical Raman spectra for a bare leaf (control) and the ink on a leaf.

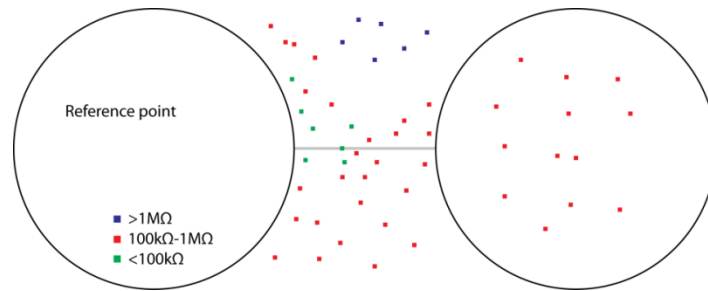
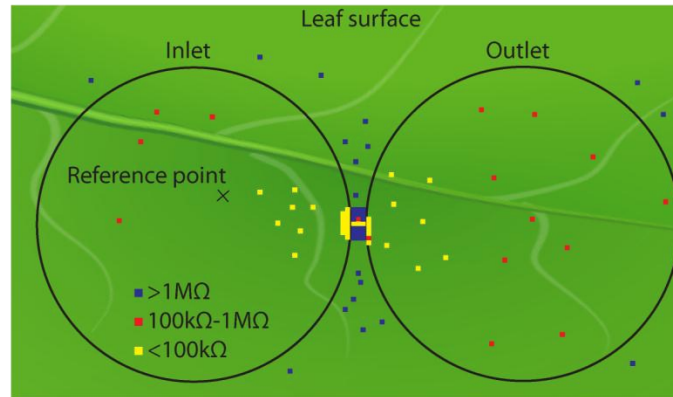


Figure S6. (top) Conductive map of leaf surface after ink printing across single stoma, showing a small conductive region in the center. For clarity, map is overlaid with sketched background. One point corresponds to $10 \times 10 \mu\text{m}^2$ region. (bottom) Conductive map demonstrating channel leaking.

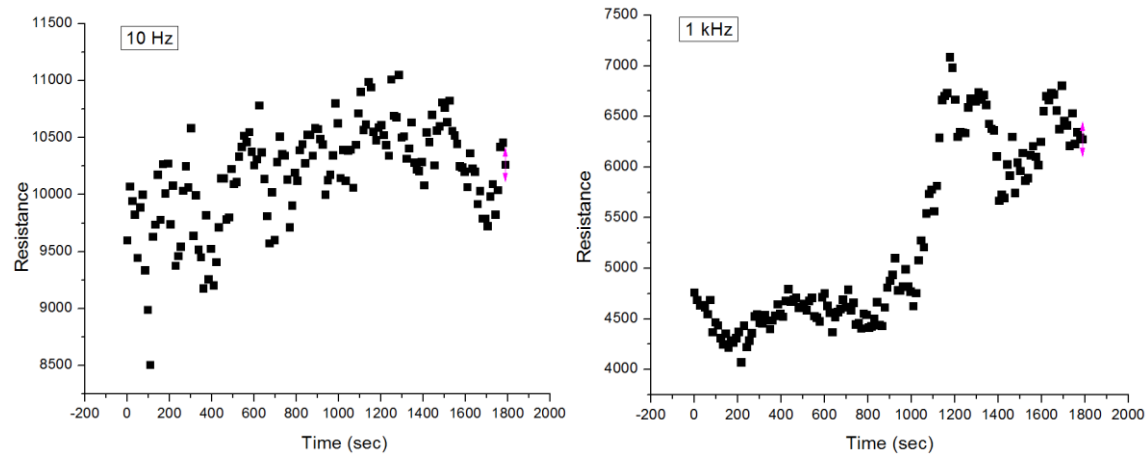


Figure S7. Examples of resistance measurements for conductive ink printed on leaf surface at different frequencies.

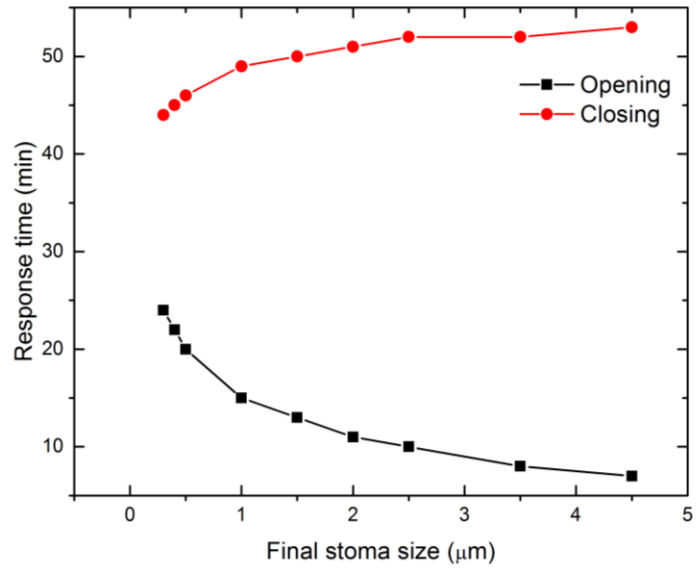


Figure S8. Calculated response time (opening and closing) for various stomatal apertures.

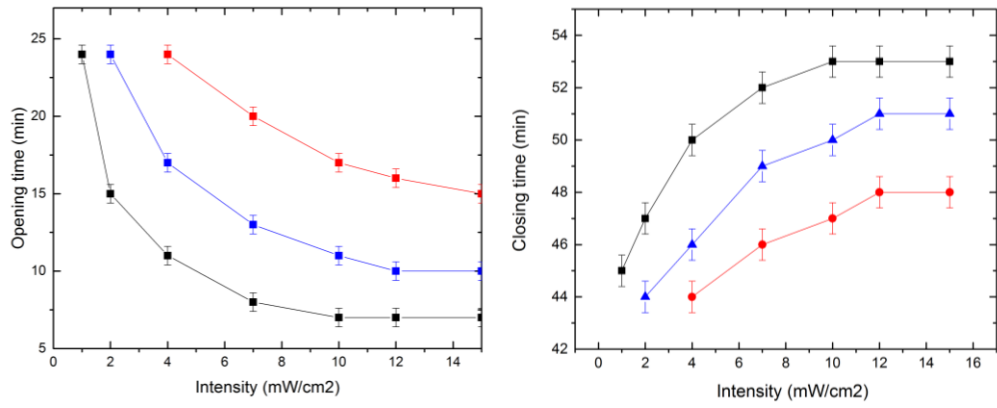


Figure S9. Calculated stomatal opening and closing times for various illumination intensities. Error bars were taken as statistical error from Fig. 2g.



Figure S10. Photograph of peace lily plant after 4 days drought period.

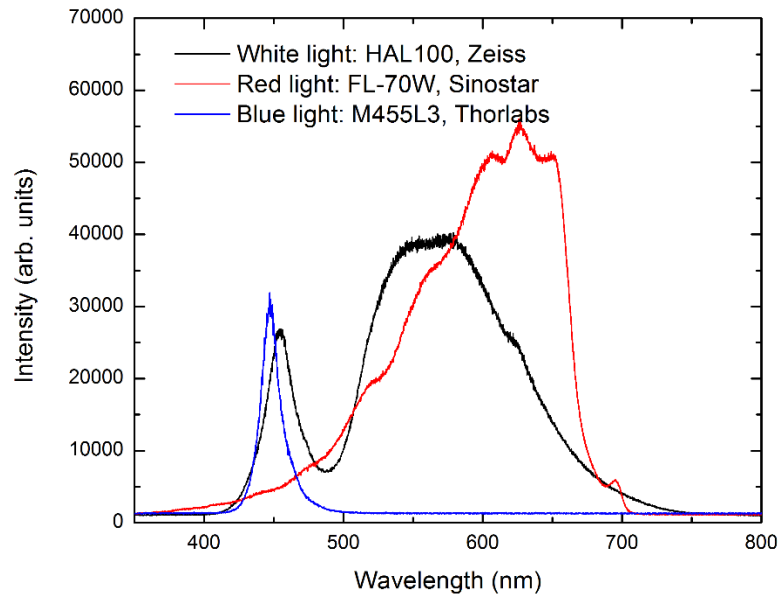


Figure S11. Lamp emission spectra for red, blue and white light sources.

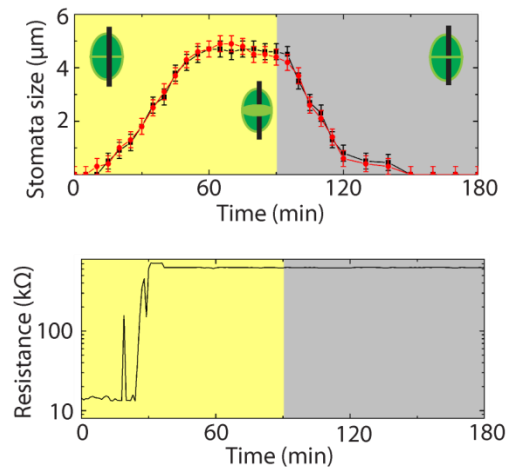


Figure S12. (Top) Stomatal dynamics when the plant is illuminated with a white light for 90 min and then put in the dark (black: stoma with printed ink, red: stoma without ink, $I=10 \text{ mW/cm}^2$). Insets show unbroken ink wire across stoma, broken wire after stoma opens and broken wire when stoma closes (from left to right). (Bottom) Resistance dynamics across the stoma with conditions as in (Top).

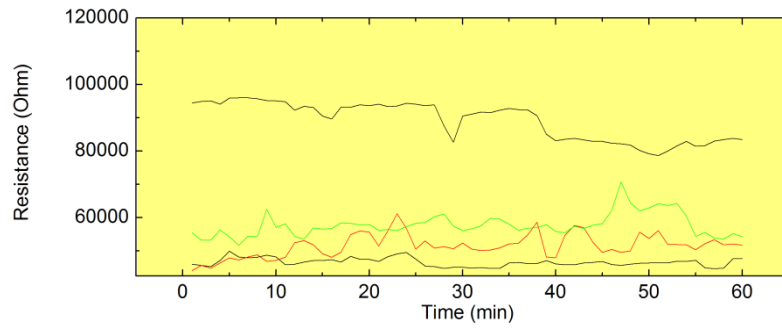


Figure S13. Resistance dynamics for stomata with printed ink without micropillars (white light, $I=10 \text{ mW/cm}^2$). For the majority of cases, stomata resistance did not change during illumination.

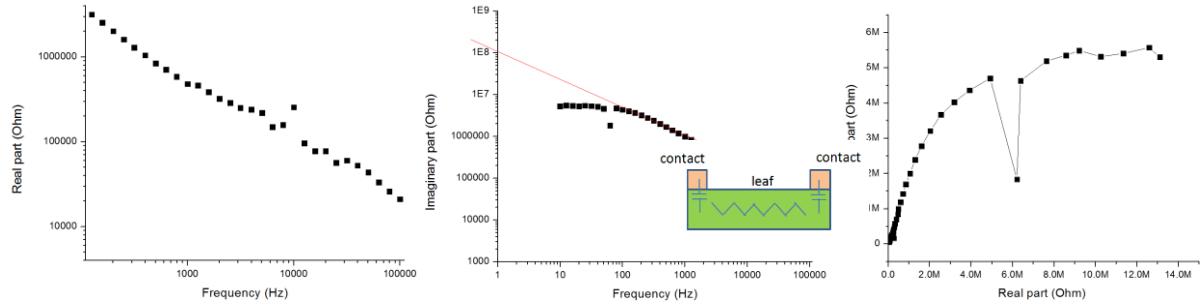


Figure S14. Impedance spectroscopy on a bare leaf. Inset shows proposed effective elements: resistive mesophyll and interlayer capacitors between mesophyll and epidermis.

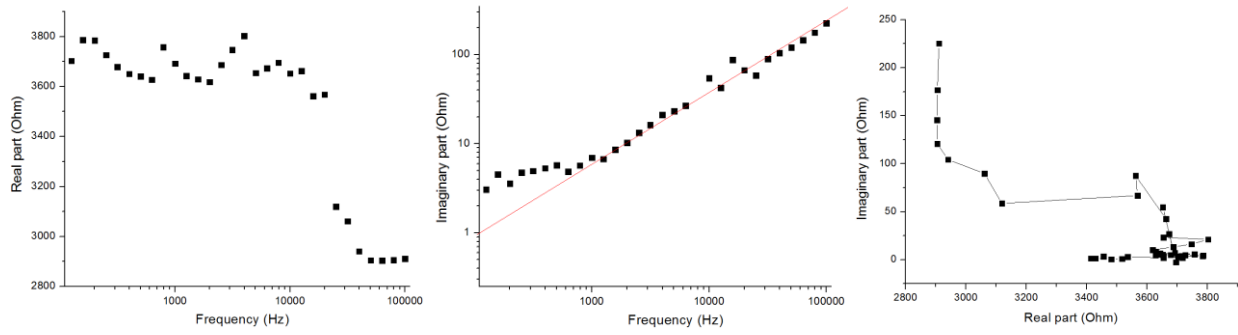


Figure S15. Impedance spectroscopy on a leaf printed with conductive ink.

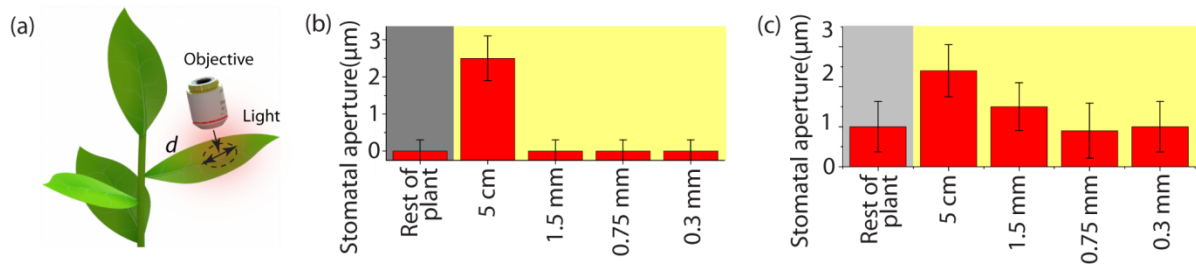


Figure S16. (a) Schematics of light illuminating limited leaf area. (b) Change in stomata size when part of the plant is illuminated with dual light for 1h ($I=7 \text{ mW/cm}^2$), while the rest of the plant is kept in the dark ($n=10$). (c) Same as (b), but the rest of plant is kept under ambient illumination ($I=3 \text{ mW/cm}^2$, $n=10$).

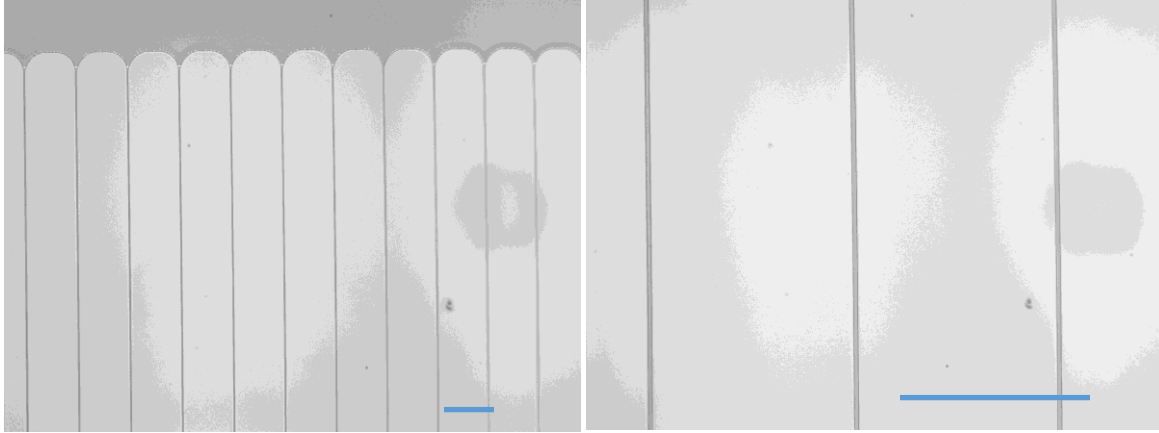


Figure S17. Optical microscope images of SU-8 electrodes. Scale bars: 100um.

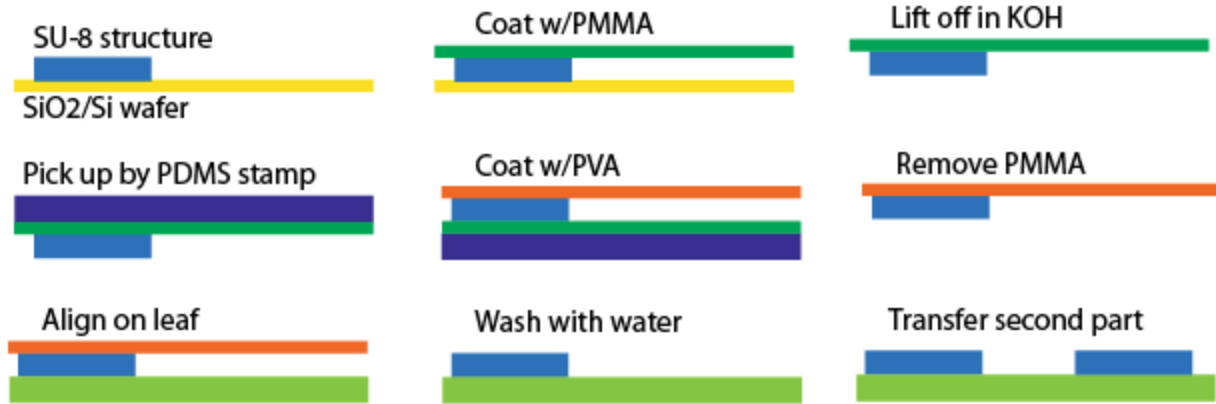


Figure S18. Schematic procedure for transferring and aligning SU-8 electrodes onto leaf surface. SU-8 structures are fabricated using photolithography and then coated with conductive ink.

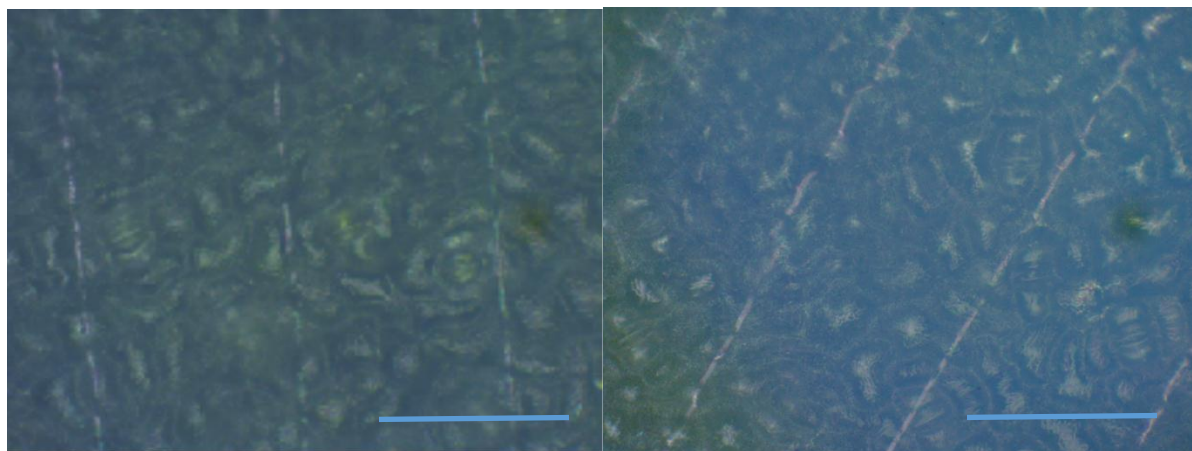


Figure S19. Optical microscope images of long SU-8 electrodes across leaf surface. Scale bars: 100 μm .

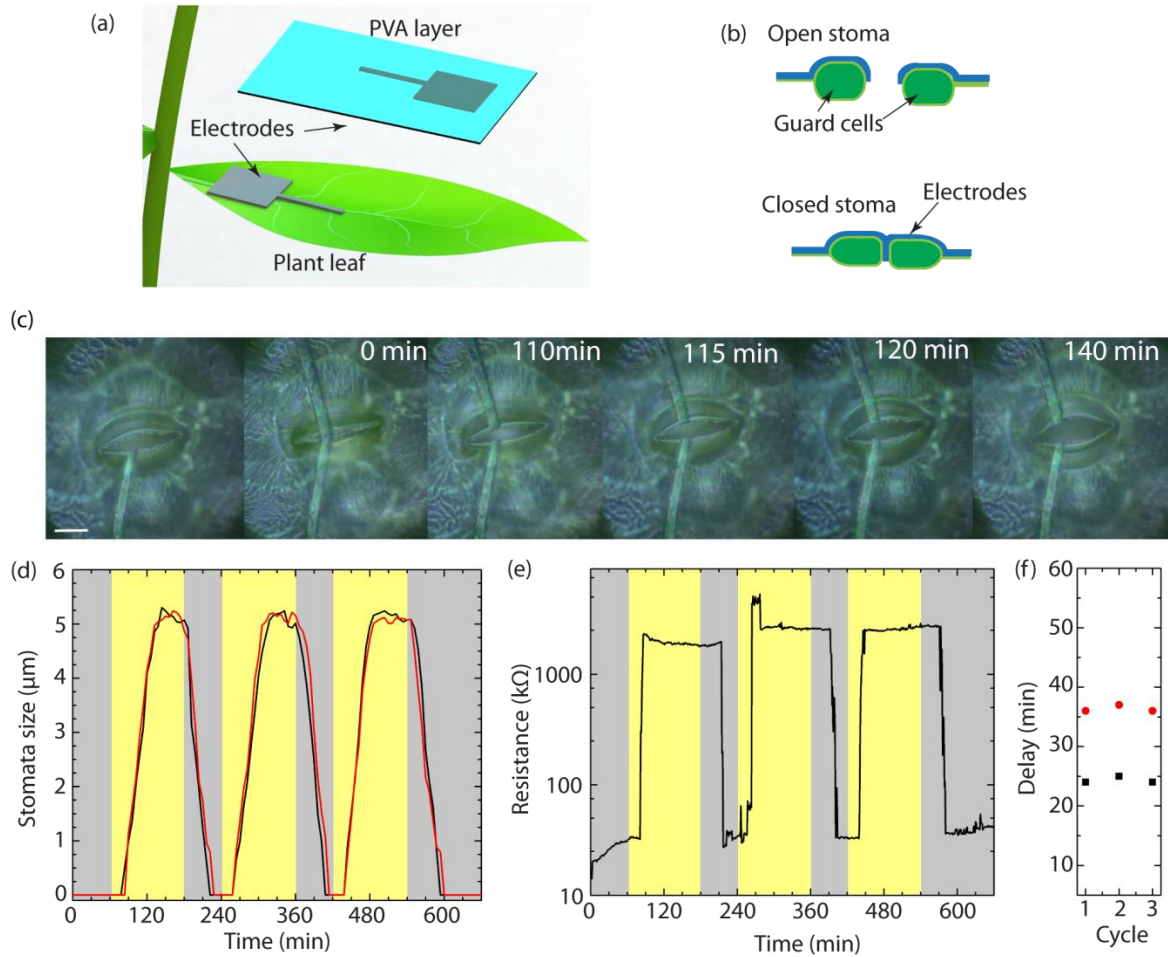


Figure S20. (a) Schematic of electrode transfer onto a leaf surface: Two electrodes are sequentially aligned on a stoma. Once an electrode is aligned and placed on a leaf, the supporting poly (vinyl) alcohol (PVA) layer is washed away with water, releasing the electrode. (b) Schematic of the electrode conformal contact with a leaf surface. (c) Set of microscope images showing two electrodes aligned on top of a stoma. The stoma opens in response to white light illumination ($I=10 \text{ mW/cm}^2$ starting at $t=60$ min). Scale bar: $10 \mu\text{m}$. (d) Optically measured stomatal aperture dynamics for a stoma with electrodes (black) and a bare stoma (red) in 3 consecutive white light on/off cycles of ($I=10 \text{ mW/cm}^2$). Error bars are omitted for clarity. (e) Simultaneous resistance dynamics of wired stomata from (d). (f) Time delay for stomata opening (black squares) and closing (red circles) for light cycles in (d).

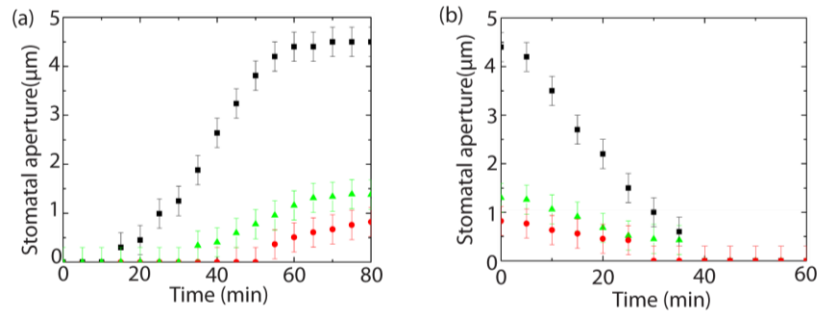


Figure S21. (a) Optically measured stomatal aperture opening dynamics for well-watered plant (black), 4 (green) and 6 (red) days long drought periods (white light $I=10 \text{ mW/cm}^2$), demonstrating the retarded stomata response during drought. (b) Stomatal closing dynamics for conditions as in (a).

1. Cañamero, R.C., et al., *Use of Confocal Laser as Light Source Reveals Stomata-Autonomous Function*. PLoS ONE, 2006. **1**(1): p. e36.
2. Savvides, A., D. Fanourakis, and W. van Ieperen, *Co-ordination of hydraulic and stomatal conductances across light qualities in cucumber leaves*. Journal of Experimental Botany, 2011.
3. Mott, K.A. and T.N. Buckley, *Patchy stomatal conductance: emergent collective behaviour of stomata*. Trends in Plant Science, 2000. **5**(6): p. 258-262.
4. Hedrich, R., et al., *Malate-sensitive anion channels enable guard cells to sense changes in the ambient CO₂ concentration*. The Plant Journal, 1994. **6**(5): p. 741-748.
5. Brearley, J., A.M. Venis, and R.M. Blatt, *The effect of elevated CO₂ concentrations on K⁺ and anion channels of Vicia faba L. guard cells*. Planta, 1997. **203**(2): p. 145-154.